

# Local composition controls pattern formation in conserved active emulsions

Florian Raßhofer<sup>1</sup> and Erwin Frey<sup>1,2,\*</sup>

<sup>1</sup>*Arnold Sommerfeld Center for Theoretical Physics and Center for NanoScience, Department of Physics, Ludwig-Maximilians-Universität München, Theresienstraße 37, D-80333 Munich, Germany*

<sup>2</sup>*Max Planck School Matter to Life, Hofgartenstraße 8, D-80539 Munich, Germany*

(Dated: March 19, 2026)

Phase separation in passive systems leads to uncontrolled droplet growth, limiting structural control in soft materials and cells. We identify a generic mechanism to arrest coarsening based on chemical interconversion between molecular species with different diffusivities. Sharp-interface theory and simulations show that when the faster-diffusing species becomes enriched inside droplets, composition gradients emerge that oppose mass influx. This transport asymmetry stabilizes droplet sizes even without interaction asymmetries, offering a minimal route to regulate structure formation in active emulsions.

Phase separation is a fundamental organizing principle in soft-matter and biological systems, from synthetic emulsions [1] and polymer blends [2], to whole ecosystems [3]. It occurs when short-range interactions favor local (self-)association over mixing, causing multi-component systems to demix into coexisting phases. In the absence of external driving and long-range interactions [4–8], phase-separated domains inevitably coarsen: Larger domains grow at the expense of smaller ones through diffusive mass exchange. This unregulated growth, known as *Ostwald ripening* [9–11], is driven by interfacial tension and constrains structural control in both materials and living systems.

This limitation has received renewed attention with the discovery of biomolecular condensates [12, 13]. These membraneless organelles participate in essential biological processes, including midcell localization [14, 15], carbon fixation [16, 17], ribosome assembly [18], and the pathology of several diseases [19, 20]. While they are believed to form via liquid–liquid phase separation [21–23], the spontaneous emergence and unregulated growth predicted by passive phase separation are difficult to reconcile with the precise spatial and temporal control required in cells. This suggests that living systems employ active mechanisms to regulate condensate formation and morphology [24, 25].

One class of mechanisms involves chemical reactions that modify phase behavior [26–30], giving rise to stable droplet sizes [31–37], droplet self-propulsion [38–41], division [42], and persistent capillary waves [43]. Previous studies have mostly examined reactions that modulate component interactions [32, 33], e.g., through post-translational modifications [44–46]. Here, we introduce a distinct form of active regulation: *Interconversion between molecular states of different diffusivity*.

Such conversion is known to drive pattern formation in dilute (mass-conserving) reaction–diffusion [(Mc)RD] systems [47–50], and has been linked to the emergence of thermophoretic fluxes [51]. However, its consequences for dense, interacting mixtures remain largely unexplored [52–54]. A key open question is whether con-

version between states of unequal diffusivity can arrest coarsening in systems with strong interactions. To address this, we study an incompressible ternary mixture of two solutes, A and B, and a solvent S; a generalization to arbitrary numbers of components is discussed in Ref. [55]. The solutes are assumed thermodynamically equivalent—sharing identical interactions and internal energies—but differ in diffusivity, and interconvert through chemical reactions. This minimal model extends classical two-component McRD systems [48, 50] to the regime of strong interactions, enabling us to disentangle the roles of short-range interactions and mobility regulation.

Combining finite-element (FEM) simulations, linear stability analysis, and sharp-interface theory, we identify two distinct pattern-forming regimes: When pairwise interactions are too weak to induce phase separation, patterns emerge solely via a generalized *mass-redistribution instability* [49, 50] and ultimately coarsen into a single dense domain. In contrast, when interactions favor phase separation, coarsening can be arrested if chemical activity locally enriches the faster diffusing species within high-density domains. This identifies a previously unrecognized mechanism by which chemical activity can arrest coarsening solely through driven transport asymmetries. Detailed calculations and further results on phase-coexistence outside the arrested regime are presented in Ref. [55].

*Model.* In thermodynamic equilibrium, the statistical properties of the mixture are described by a Flory-Huggins free energy  $\mathcal{F}$  [56–58], which depends on the local volume fractions  $\phi_{A/B}$ . Introducing the conserved *solute volume fraction*  $\rho = \phi_A + \phi_B$ , and the *local composition*  $s = (\phi_A - \phi_B)/(\phi_A + \phi_B)$ , one finds [55]

$$\mathcal{F}[\rho, s] = \frac{k_B T}{\nu} \int d\mathbf{r} \left[ \frac{\tilde{\kappa}}{2} (\nabla \rho)^2 + f(\rho) + \rho g(s) \right], \quad (1)$$

where we assume that all components occupy the same molecular volume  $\nu$ . For brevity, we occasionally refer to  $\rho$  as the solute density, although it denotes a volume fraction. The first two terms in Eq. (1) describe a sym-

metric binary mixture: Density gradients are penalized by a stiffness coefficient  $\tilde{\kappa}$ , and the local free energy density  $f(\rho) = \rho \log(\rho) + (1 - \rho) \log(1 - \rho) + \chi \rho(1 - \rho)$  includes entropic and energetic contributions, with  $\chi$  denoting the Flory–Huggins parameter [56]. For  $\chi > 2$ ,  $f(\rho)$  becomes non-convex, and the system separates into coexisting phases characterized by the local minima  $\rho_{\pm}$  of  $f(\rho)$ . The last term,  $\rho g(s)$ , describes the entropy of mixing between A and B particles. The function  $g(s) = \frac{1+s}{2} \log\left(\frac{1+s}{2}\right) + \frac{1-s}{2} \log\left(\frac{1-s}{2}\right)$  is strictly convex, ensuring thermodynamic stability against compositional fluctuations.

In the absence of chemical reactions, relaxation towards thermodynamic equilibrium follows the principles of non-equilibrium thermodynamics [59, 60]. Each species  $i \in \{A, B\}$  satisfies a continuity equation with diffusive flux  $\mathbf{J}_i = -M_i(\{\phi_j\}) \nabla \bar{\mu}_i$ , where  $\bar{\mu}_i = \nu \delta \mathcal{F} / \delta \phi_i$  denote the exchange chemical potentials. Neglecting cross-diffusion [55], we choose effective mobilities  $M_i = D_i \phi_i (1 - \rho)$ , to recover Fick’s law with constant  $D_i$  in the dilute, non-interacting limit.

In addition, we include local interconversion  $B \rightleftharpoons A$  with rates  $k_{\rightarrow}$  and  $k_{\leftarrow}$ , giving rise to a reactive flux  $\bar{\mathcal{R}} = k_{\rightarrow} \phi_B - k_{\leftarrow} \phi_A$ . Unless stated otherwise, we choose  $k_{\rightarrow} = \rho / \tau$  and  $k_{\leftarrow} = \rho_0 / \tau$ , where  $\tau$  sets the reaction timescale, and  $\rho_0 = 0.5$  is fixed throughout the manuscript. This yields a unique steady-state composition  $\bar{s}(\rho) = (\rho - \rho_0) / (\rho + \rho_0)$ , implying enrichment of A in dense regions ( $\partial_{\rho} \bar{s} > 0$ ), breaking the inherent  $A \leftrightarrow B$  symmetry of the free energy [Eq. (1)]. Such density-enhanced  $B \rightarrow A$  conversion may arise from crowding-induced conformational switching [61, 62], phase-specific catalysis [63, 64], or active mobility regulation [65, 66]. Our results, however, do not rely on this specific parametrization: Any rate law that generates a unique, stable, and monotonic fixed point  $\bar{s}(\rho)$  produces the same qualitative behavior.

To identify the relevant control parameters, we nondimensionalize space and time as  $\mathbf{r} \rightarrow a \mathbf{r}$  and  $t \rightarrow (a^2 / \bar{D}) t$ , using the particle diameter  $a = \nu^{1/d}$  and the mean diffusivity  $\bar{D} = (D_A + D_B) / 2$  as natural units. The resulting dimensionless equations read [55]

$$\partial_t \rho = \nabla \cdot \{M(\rho)(1 + Ds) \nabla [\mu + \log(1 + Ds)]\}, \quad (2a)$$

$$\partial_t [s\rho] = \nabla \cdot \{M(\rho)[(D + s) \nabla \mu + \nabla s]\} + \frac{\mathcal{R}(\rho, s)}{\ell^2}, \quad (2b)$$

with  $M(\rho) = \rho(1 - \rho)$ , the binary chemical potential  $\mu = -\kappa \nabla^2 \rho + f'(\rho)$  ( $\kappa = \tilde{\kappa} a^{-2}$ ), and  $\mathcal{R} = \tau \bar{\mathcal{R}}$ . Two dimensionless parameters capture the departure from ordinary mixture dynamics: The diffusivity contrast  $D = (D_A - D_B) / (D_A + D_B)$  encodes how transport asymmetry biases mass-fluxes away from the case of a binary mixture, which is recovered for  $D = 0$ . The parameter  $\ell^2 = \tau \bar{D} / (2a^2)$  compares the typical diffusion length during a reaction time,  $\ell_{\tau}^2 \sim \tau \bar{D}$ , to the micro-

scopic particle size  $a$ , setting the characteristic (dimensionless) length scale over which the composition field responds to local density variations.

*Limiting behavior.* In the absence of chemical activity, or when reactions satisfy detailed balance [55], the steady state is characterized by uniform composition ( $\nabla s = 0$ ) and chemical potential ( $\nabla \mu = 0$ ). Consequently, phase coexistence is governed by the equilibrium conditions of a binary mixture.

In the fast-reaction limit ( $\ell \ll 1$ ), local composition relaxes instantaneously to its reactive steady state,  $s = \bar{s}(\rho)$ , allowing for adiabatic elimination. In this case,  $\rho$  obeys conserved gradient dynamics  $\partial_t \rho = \nabla \cdot \{M(\rho)[1 + D\bar{s}(\rho)] \nabla \mu_{\text{eff}}\}$ , where the effective chemical potential  $\mu_{\text{eff}} = \delta \mathcal{F}_{\text{eff}} / \delta \rho$  follows from the free energy functional [55]

$$\mathcal{F}_{\text{eff}}[\rho] = \int d\mathbf{r} \left\{ \frac{\kappa}{2} (\nabla \rho)^2 + f(\rho) + \int^{\rho} \log[1 + D\bar{s}(\bar{\rho})] \right\}. \quad (3)$$

Despite being out of equilibrium, the dynamics map to an effective binary mixture whose chemical potential is corrected by a term  $\log[1 + D\bar{s}(\rho)]$ . Hence, genuinely non-equilibrium behavior arises only for intermediate activity levels.

*Stability.* Linear stability analysis of the homogeneous steady state  $(\bar{\rho}, \bar{s})$  yields a dispersion relation with two branches,  $\sigma_{\pm}(q)$ , which satisfy  $\sigma_{+} \geq \sigma_{-}$ ,  $\forall q$ , and are real-valued over nearly the entire parameter range; complex eigenvalues only occur in a narrow, linearly stable regime [55]. As detailed in Fig. 1(a), a long-wavelength (type-II) pattern-forming instability [67] occurs when [55]

$$[1 + D\bar{s}(\bar{\rho})] f''(\bar{\rho}) < -D \partial_{\rho} \bar{s}(\bar{\rho}), \quad (4)$$

generalizing the mass-redistribution instability known from two-component McRD systems [48, 50]. Without chemical activity or for equal diffusivities ( $D = 0$ ), the condition reduces to the classical spinodal criterion  $f''(\bar{\rho}) < 0$  for phase separation in a binary mixture [56, 68].

The instability condition, Eq. (4), reflects a competition between composition-driven and chemical-potential-driven fluxes [Fig. 1(d,e)]: To illustrate this, consider a small local density increase above the homogeneous state. This shifts local chemical equilibrium, inducing a change in composition, which has the same sign as the density change [ $\partial_{\rho} \bar{s} > 0$ , Fig. 1(e)]. The resulting composition gradient drives a mass flux  $-DM(\rho) \nabla s \approx -DM(\bar{\rho}) \partial_{\rho} \bar{s} \nabla \rho$  [Eq. (2a)]. If A diffuses more slowly ( $D < 0$ ), the flux points up the density gradient and amplifies the perturbation [Fig. 1(d)]. In contrast, outside the spinodal regime [ $f''(\bar{\rho}) > 0$ ], chemical potential gradients drive a restoring flux with a positive effective diffusion constant  $M(1 + D\bar{s}) f''(\bar{\rho})$  [Eq. (2a)]. Instability sets in when the composition-driven influx dominates, i.e., when Eq. (4) holds. Conversely, if

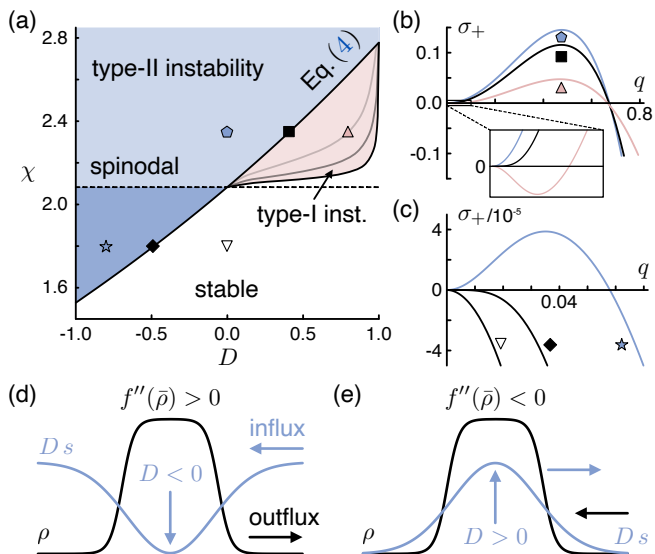


FIG. 1. **Linear stability analysis.** The homogeneous steady state is stable (white) or displays a type-I (red/light gray) or type-II (blue/gray) instability. (a) Stability diagram as a function of  $D$  and  $\chi$  for fixed  $\bar{\rho} = 0.4$ ,  $d = 2$ , and  $\ell \in \{5, 10, 20\}$  (light gray, gray, and black lines). In the presence of driven chemical reactions, the boundary of the type-II regime (black line) is determined by Eq. (4). In the equilibrium limit, a homogeneous state is linearly unstable above the (dashed) spinodal line  $\chi = 1/[2\bar{\rho}(1 - \bar{\rho})]$ . (b, c) Upper branch of the dispersion relation,  $\sigma_+(q)$ , for parameters corresponding to the different markers in subpanel (a) and  $\ell = 20$ . (d, e) Composition weighted diffusivity  $Ds$  (blue/gray) for a weakly perturbed homogeneous density  $\rho$  (black). Horizontal arrows indicate composition- (blue/gray) and chemical-potential-driven (black) fluxes, respectively.

the faster-diffusing species accumulates in dense regions [ $D \partial_{\rho} \bar{s} > 0$ , Fig. 1(e)], composition-driven fluxes oppose mass accumulation, and a type-II instability is only possible within the spinodal regime [ $f''(\bar{\rho}) < 0$ ].

When the mass-redistribution criterion [Eq. (4)] is not satisfied, long-wavelength modes remain stable. Simultaneously, interfacial stiffness  $\kappa$  suppresses short-wavelength fluctuations, leaving only an intermediate wavenumber interval in which modes can grow for sufficiently strong interactions [large  $\chi$ , Fig. 1(a, b)]. Unlike the type-II criterion [Eq. (4)], which is independent of the diffusive length scale  $\ell$ , the onset of this type-I instability depends on  $\ell$  [Fig. 1(a)]. This reflects their different physical origins: Type-II instabilities are purely diffusive, governed by  $\mathcal{O}(q^2)$  terms in the dispersion relation, whereas type-I instabilities require a sign change in the higher-order  $\mathcal{O}(q^4)$  term, which depends on  $\ell$  [55].

*Phase diagram.* To explore the nonlinear dynamics, we performed FEM simulations over a broad parameter range [69]. Within the linearly unstable region, the outcome depends sensitively on the diffusivity contrast (Fig. 2): For  $D \leq 0$ , the system invariably coarsens

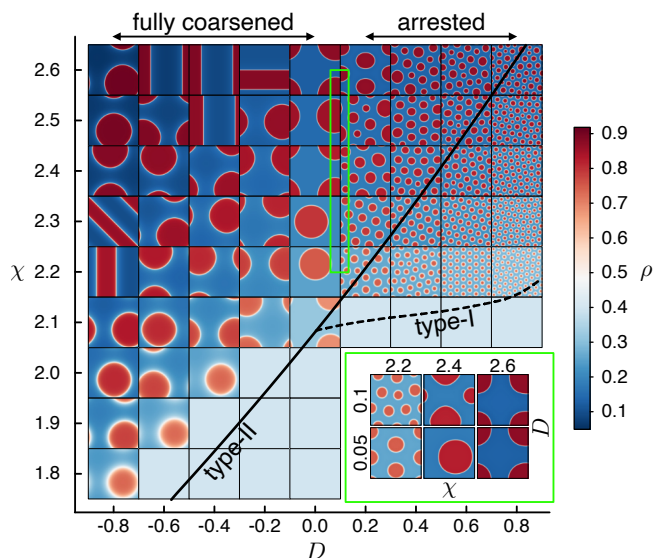


FIG. 2. **Phase diagram.** Snapshots of the conserved density  $\rho$  at time  $t = 10^8/(1 + D)$ , obtained from FEM simulations in a square domain of size  $L = 200$  with periodic boundary conditions. The system is initialized with small perturbations around the homogeneous steady state. Color indicates local density (colorbar); in grayscale renderings, interfaces appear white. The inset shows snapshots for  $D \leq 0.1$  (green box). Dashed and solid lines mark the boundaries of the type-I and type-II unstable regimes, respectively (Fig. 1). All simulations use  $\ell = 20$  and the other parameters as in Fig. 1.

into macroscopic phase separation, whereas for  $D > 0$  complete phase separation occurs only in a narrow region  $D \lesssim 0.1$ ; at larger  $D$  the system settles into an *ensemble of coexisting finite-size droplets*.

While arrested coarsening is typically expected near the onset of a type-I instability [70], we observe that enrichment of the faster-diffusing species in dense regions robustly arrests coarsening even within the type-II unstable regime, provided phase separation is driven by pairwise interactions ( $\chi > 2$ ). In contrast, when pattern formation is driven by composition gradients and opposed by chemical-potential fluxes, no stable finite-size structures emerge: As shown in Fig. 2, transient patterns can still emerge in the thermodynamically stable regime ( $\chi \leq 2$ ) via the generalized mass-redistribution instability [Eq. (4)]. However, as for dilute two-component McRD systems [71, 72], these patterns invariably coarsen, regardless of the specific reaction kinetics  $\mathcal{R}$  [69]. This shows that coarsening arrest requires attractive short-range interactions combined with opposing fluxes from active composition gradients—not the reverse.

*Arrested coarsening.* To uncover the mechanism of arrested coarsening, we consider a dilute solution where droplets are well separated and interact only through the common far-field density  $\rho_{\infty}$ . In this limit, the dynamics reduce to those of an isolated spherical droplet in a homogeneous background. Coarsening is arrested

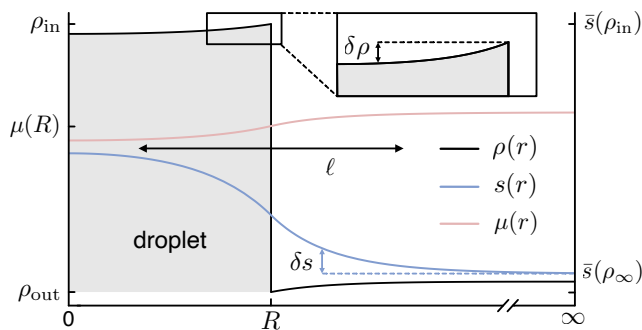


FIG. 3. **Sharp-interface limit** for an isolated droplet. An infinitely sharp interface at  $r = R$  separates the high-density interior (gray) from the low-density exterior (white). Within each domain, the solute density  $\rho$  (black) and chemical potential  $\mu$  (red/light gray) remain close to their equilibrium values  $\rho_{\text{in/out}}$  and  $\mu(R)$ . The composition  $s$  (blue) varies on a characteristic length scale  $\ell$ , and relaxes towards chemical equilibrium in the far field [ $s \rightarrow \bar{s}(\rho_\infty)$ ].

if Eq. (2) admits a stable steady-state solution at finite droplet radius  $R$ . If no such fixed point exists, droplets dissolve ( $R \rightarrow 0$ ) or grow without bound ( $R \rightarrow \infty$ ).

The local solute flux  $\mathbf{J}_\rho = -M(\rho)(1 + Ds)\nabla\eta$  [Eq. (2a)] is governed by the mass-redistribution potential  $\eta(\mathbf{r}) \equiv \mu(\mathbf{r}) + \log[1 + Ds(\mathbf{r})]$ . In steady state, vanishing mass flux requires  $\nabla\eta = 0$ . Evaluating this condition at the droplet interface and in the far-field yields

$$\mu_\infty - \mu(R) = \log[1 + Ds(R)] - \log[1 + Ds_\infty], \quad (5)$$

where  $\mu_\infty = f'(\rho_\infty)$  and  $s_\infty = \bar{s}(\rho_\infty)$  are set by local thermodynamic and chemical equilibrium. Equation (5) shows that a finite droplet size can be maintained only if the chemical potential difference is exactly balanced by a change in local composition. Since  $\mu(R)$  and  $s(R)$  depend on the stationary profiles, determining this balance requires the full solution for  $\rho(r)$  and  $s(r)$ .

*Sharp interface limit.* Steady-state solutions of Eq. (2) can be obtained in the asymptotic regime ( $w \ll R, \ell$ ), where the interfacial width  $w$  is negligible compared with the droplet radius  $R$  and the diffusive length scale  $\ell$  (Fig. 3). This scale separation allows for several simplifications:

(i) Across the narrow interface, the composition is nearly uniform ( $\nabla s \approx 0$ ). Stationarity ( $\nabla\eta = 0$ ), then, implies  $\nabla\mu \approx 0$ , i.e., local thermodynamic equilibrium. Consequently, the interfacial chemical potential  $\mu(R)$  and the coexisting densities  $\rho_{\text{in/out}}$  adjacent to the interface (Fig. 3) are determined by a standard common-tangent construction [55, 68].

(ii) The droplet interior and exterior can be treated as quasi-homogeneous compartments, with only small density variations (Fig. 3). Accordingly, we linearize the steady-state equations [Eq. (2)] around the equilibrium coexistence densities,  $\rho = \rho_{\text{in/out}} + \delta\rho$ , imposing

$\delta\rho(R) = 0$  at the interface. Linearization of the composition field  $s$  is more subtle: For large droplets ( $R \gg \ell$ ),  $s$  varies between the two reactive equilibria at the droplet center [ $s \approx \bar{s}(\rho_{\text{in}})$ ] and in the far-field [ $s \approx \bar{s}(\rho_\infty)$ ]. Thus, compositional variations  $\delta s \approx \mathcal{O}[\bar{s}(\rho_{\text{in}}) - \bar{s}(\rho_\infty)]$  are generally not small. In contrast, for small droplets ( $R \ll \ell$ ), the composition inside the droplet cannot fully relax to chemical equilibrium and instead remains nearly uniform throughout the system; see Fig. 3. In this limit, we write  $s \approx s_\infty + \delta s$  and expand Eq. (2) to leading order in  $\delta s$ . Detailed validity bounds and alternative linearization schemes are discussed in Ref. [55].

(iii) Finally, we use the stationarity condition,  $\eta(\delta\rho, \delta s) = \mu_\infty + \log(1 + Ds_\infty)$ , which links compositional and density variations, to eliminate  $\delta\rho$ . To leading order in  $\delta s$ , the steady-state equations [Eq. (2)] then reduce to a set of piecewise-linear differential equations

$$K_\alpha \nabla^2 \delta s_\alpha(r) + \frac{K_\alpha}{\ell_\alpha^2} [\delta s_\alpha^0 - \delta s_\alpha(r)] = 0, \quad (6)$$

where  $K_\alpha$  and  $\ell_\alpha$  with  $\alpha \in \{\text{in}, \text{out}\}$  denote the region-specific mobility and screening length. While the outer offset  $\delta s_{\text{out}}^0 = 0$  vanishes ( $s \rightarrow s_\infty$  as  $r \rightarrow \infty$ ), the inner offset  $\delta s_{\text{in}}^0$  characterizes the composition shift at the center of a large droplet ( $R \gg \ell_{\text{in}}$ ) [55].

Solutions to Eq. (6), are obtained by enforcing regularity at the origin ( $\partial_r s|_{r=0} = 0$ ), and matching the density to its far-field value [ $\lim_{r \rightarrow \infty} \rho(r) = \rho_\infty$ ]. Integration across the interface further imposes flux continuity:  $K_{\text{in}} \partial_r \delta s_{\text{in}}(R) = K_{\text{out}} \partial_r \delta s_{\text{out}}(R)$ . This yields a nonlinear self-consistency condition for the stationary radius  $R$ , which is solved numerically [69].

Explicit calculation steps and analytical results are presented in Ref. [55]. Depending on the far-field density  $\rho_\infty$ , and the diffusivity contrast  $D$ , one finds either one, two, or no steady-state solutions (Fig. 4). Here, we focus on the supersaturated case ( $\rho_\infty > \rho_-$ ), for which droplet growth occurs in an equilibrium mixture [68]; the undersaturated scenario is discussed in Ref. [55].

In the equilibrium limit ( $D = 0$ ), the system admits a single stationary solution (Fig. 4) at the critical nucleation radius  $R_c$  of a binary mixture, which corresponds to an unstable fixed point [68]. For increasing diffusivity contrast  $D$ , this solution persists with little change, showing that the nucleation barrier is only weakly affected by the non-equilibrium drive. Beyond a critical threshold  $D_c$ , a second stationary solution emerges (Fig. 4), corresponding to a stable droplet of finite size. The onset of this arrested regime can be estimated as [55]

$$D_c = \frac{f''(\rho_-)(\rho_\infty - \rho_-) \left(1 + \sqrt{\frac{\partial_s \mathcal{R}|_{\text{out}}}{\partial_s \mathcal{R}|_{\text{in}}}}\right)}{(\partial_s \log \mathcal{R}|_{\text{out}})^{-1} - (\partial_s \log \mathcal{R}|_{\text{in}})^{-1}}, \quad (7)$$

where  $|_{\text{in/out}}$  denotes evaluation at  $(\rho_\pm, s_\infty)$ . Equation (7) shows that stronger supersaturation requires a

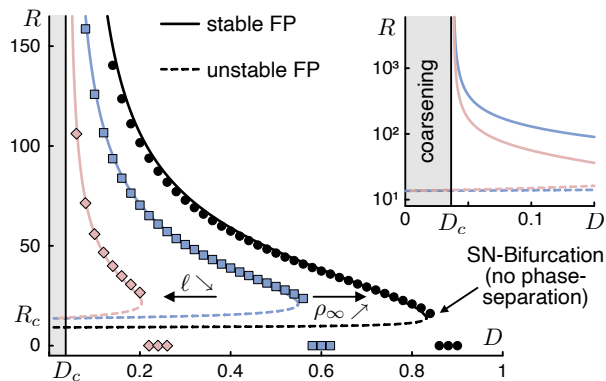


FIG. 4. **Single droplet steady states** in a supersaturated solution. Stable (solid) and unstable (dashed) stationary radii obtained from sharp-interface theory and FEM simulations (bullets) in a three-dimensional ( $d = 3$ ) spherically symmetric system ( $L = 15\ell$ ) [69] for  $\chi = 2.4$  ( $\rho_- = 0.17$ ), and  $\{\rho_\infty, \ell\} = \{0.185, 200\}$  (black),  $\{0.18, 200\}$  (blue/gray),  $\{0.18, 100\}$  (red/light gray). The inset shows the asymptotic behavior near the onset  $D_c$  of arrested coarsening [Eq. (7)].

larger diffusivity contrast to arrest coarsening, while the denominator quantifies the asymmetry of the reaction’s sensitivity to composition changes inside versus outside the droplet, with greater asymmetry lowering the threshold. At  $D = D_{SN}$ , which increases with  $\rho_\infty$  and decreases with  $\ell$ , both fixed points vanish in a saddle–node (SN) bifurcation, signaling complete suppression of phase separation (Fig. 4).

Comparison with FEM simulations of a three-dimensional spherical droplet [69] shows quantitative agreement for both the steady droplet radius and the onset of arrested coarsening (Fig. 4). Only for stronger supersaturation and near the saddle-node bifurcation, the sharp-interface theory weakly deviates from the FEM results. These discrepancies correlate with larger  $D$  and  $\rho_\infty$ , which drive the density profile away from the equilibrium plateau values  $\rho_{in/out}$ , indicating the gradual breakdown of our linearization scheme.

*Conclusions.* We have shown that interconversion between molecular states of different diffusivity—but identical interactions—can arrest coarsening when the faster species is enriched in dense regions. Crucially, the resulting droplet size is not set by the wavelength of a pattern-forming instability, but emerges from a balance of mass fluxes driven by chemical potential and composition gradients [Eq. (5)].

This mechanism differs from established models of coarsening arrest in dense interacting mixtures, which rely on reactions converting between strongly interacting and freely diffusing species [32, 33, 73]. In practice, chemical modifications of the solutes likely affect both mobility and interactions, making it challenging to isolate one effect from the other. However, mobility regulation may be particularly relevant for membrane-associated

phase separation [74, 75], where protein mobility depends on the number of anchors [76, 77], lipid-binding domains [78, 79], and membrane inclusion size [80, 81].

These properties could be dynamically tuned through reversible modifications, such as lipidation [82], enabling changes in mobility without substantially altering inter-particle interactions. Similar effects may also arise in the cytoplasm: Phosphorylation-regulated binding to slow-moving structures, such as RNA clusters [83], could transiently reduce molecular mobility in the bulk, offering an alternative route to mobility-dependent regulation.

From a broader perspective, our results uncover a general mechanism for regulating mesoscale organization in active mixtures: Positive feedback between local density and effective mobility can counteract coarsening and stabilize finite-size domains. An analogous feedback mechanism operates in ecological systems, where individuals increase their motility in response to local crowding and resource depletion, giving rise to self-organized clusters that resist coarsening [65, 84]. This suggests that differential mobility may represent a universal strategy for maintaining spatial structure in out-of-equilibrium systems [85, 86].

We thank Henrik Weyer and Tobias Roth for stimulating discussions and Jan Willeke and Xaver Kainz for their insightful comments on our manuscript. This research was funded by the Deutsche Forschungsgemeinschaft (DFG, German Research Foundation) under Germany’s Excellence Strategy – EXC3092 – 533751719. We further acknowledge support from the John Templeton Foundation, and the U.S. National Science Foundation (NSF) under Grant No. PHY-2309135 through the Kavli Institute for Theoretical Physics (KITP).

\* Corresponding author: [frey@lmu.de](mailto:frey@lmu.de)

- [1] Zi Lin, Thomas Beneyton, Jean-Christophe Baret, and Nicolas Martin, “Coacervate Droplets for Synthetic Cells,” *Small Methods* **7**, e2300496 (2023).
- [2] Piotr Knychala, Ksenia Timachova, Michał Banaszak, and Nitash P. Balsara, “50th Anniversary Perspective: Phase Behavior of Polymer Solutions and Blends,” *Macromolecules* **50**, 3051–3065 (2017).
- [3] Koen Siteur, Quan-Xing Liu, Vivi Rottschäfer, Tjisse van der Heide, Max Rietkerk, Arjen Doelman, Christoffer Boström, and Johan van de Koppel, “Phase-separation physics underlies new theory for the resilience of patchy ecosystems,” *Proceedings of the National Academy of Sciences* **120**, e2202683120 (2023).
- [4] Fong Liu and Nigel Goldenfeld, “Dynamics of phase separation in block copolymer melts,” *Physical Review A* **39**, 4805–4810 (1989).
- [5] Sharon C. Glotzer and Antonio Coniglio, “Self-consistent solution of phase separation with competing interactions,” *Physical Review E* **50**, 4241–4244 (1994).
- [6] C. B. Muratov, “Theory of domain patterns in systems with long-range interactions of Coulomb type,” *Physical*

- Review E **66**, 066108 (2002).
- [7] Amit Kumar and Samuel A. Safran, “Fluctuations and Shape Dependence of Microphase Separation in Systems with Long-Range Interactions,” *Physical Review Letters* **131**, 258401 (2023).
  - [8] Antonia Winter, Yuhao Liu, Alexander Ziepkke, George Dadunashvili, and Erwin Frey, “Phase separation on deformable membranes: Interplay of mechanical coupling and dynamic surface geometry,” *Physical Review E* **111**, 044405 (2025).
  - [9] W. Ostwald, “Studien über die Bildung und Umwandlung fester Körper,” *Zeitschrift für Physikalische Chemie* **22U**, 289–330 (1897).
  - [10] Carl Wagner, “Theorie der Alterung von Niederschlägen durch Umlösen (Ostwald-Reifung),” *Zeitschrift für Elektrochemie, Berichte der Bunsengesellschaft für physikalische Chemie* **65**, 581–591 (1961).
  - [11] I.M. Lifshitz and V.V. Slyozov, “The kinetics of precipitation from supersaturated solid solutions,” *Journal of Physics and Chemistry of Solids* **19**, 35–50 (1961).
  - [12] Anthony A. Hyman, Christoph A. Weber, and Frank Jülicher, “Liquid-Liquid Phase Separation in Biology,” *Annual Review of Cell and Developmental Biology* **30**, 39–58 (2014).
  - [13] Salman F. Banani, Hyun O. Lee, Anthony A. Hyman, and Michael K. Rosen, “Biomolecular condensates: organizers of cellular biochemistry,” *Nature Reviews Molecular Cell Biology* **18**, 285–298 (2017).
  - [14] Dominik Schumacher, Silke Bergeler, Andrea Harms, Janet Vonck, Sabrina Huneke-Vogt, Erwin Frey, and Lotte Søggaard-Andersen, “The PomXYZ Proteins Self-Organize on the Bacterial Nucleoid to Stimulate Cell Division,” *Developmental Cell* **41**, 299–314.e13 (2017), 1801.09549.
  - [15] Silke Bergeler and Erwin Frey, “Regulation of Pom cluster dynamics in *Myxococcus xanthus*,” *PLoS Computational Biology* **14**, e1006358 (2018), 1801.06133.
  - [16] Tobias Wunder, Steven Le Hung Cheng, Soak-Kuan Lai, Hoi-Yeung Li, and Oliver Mueller-Cajar, “The phase separation underlying the pyrenoid-based microalgal Rubisco supercharger,” *Nature Communications* **9**, 5076 (2018).
  - [17] Shan He, Victoria L Crans, and Martin C Jonikas, “The pyrenoid: the eukaryotic CO<sub>2</sub>-concentrating organelle,” *The Plant Cell* **35**, 3236–3259 (2023).
  - [18] Marina Feric, Nilesh Vaidya, Tyler S. Harmon, Diana M. Mitrea, Lian Zhu, Tiffany M. Richardson, Richard W. Kriwacki, Rohit V. Pappu, and Clifford P. Brangwynne, “Coexisting Liquid Phases Underlie Nucleolar Subcompartments,” *Cell* **165**, 1686–1697 (2016).
  - [19] Simon Alberti and Dorothee Dormann, “Liquid-Liquid Phase Separation in Disease,” *Annual Review of Genetics* **53**, 1–24 (2019).
  - [20] Simon Alberti and Anthony A. Hyman, “Biomolecular condensates at the nexus of cellular stress, protein aggregation disease and ageing,” *Nature Reviews Molecular Cell Biology* **22**, 196–213 (2021).
  - [21] Clifford P. Brangwynne, Christian R. Eckmann, David S. Courson, Agata Rybarska, Carsten Hoege, Jöbin Gharakhani, Frank Jülicher, and Anthony A. Hyman, “Germline P Granules Are Liquid Droplets That Localize by Controlled Dissolution/Condensation,” *Science* **324**, 1729–1732 (2009).
  - [22] Steven Boeynaems, Simon Alberti, Nicolas L. Fawzi, Tanja Mittag, Magdalini Polymenidou, Frederic Rousseau, Joost Schymkowitz, James Shorter, Benjamin Wolozin, Ludo Van Den Bosch, Peter Tompa, and Monika Fuxreiter, “Protein Phase Separation: A New Phase in Cell Biology,” *Trends in Cell Biology* **28**, 420–435 (2018).
  - [23] Anatol W. Fritsch, Andrés F. Diaz-Delgadillo, Omar Adame-Arana, Carsten Hoege, Matthäus Mittasch, Moritz Kreysing, Mark Leaver, Anthony A. Hyman, Frank Jülicher, and Christoph A. Weber, “Local thermodynamics govern formation and dissolution of *Caenorhabditis elegans* P granule condensates,” *Proceedings of the National Academy of Sciences* **118**, e2102772118 (2021).
  - [24] Wilton T. Snead and Amy S. Gladfelter, “The Control Centers of Biomolecular Phase Separation: How Membrane Surfaces, PTMs, and Active Processes Regulate Condensation,” *Molecular Cell* **76**, 295–305 (2019).
  - [25] Johannes Söding, David Zwicker, Salma Sohrabi-Jahromi, Marc Boehning, and Jan Kirschbaum, “Mechanisms for Active Regulation of Biomolecular Condensates,” *Trends in Cell Biology* **30**, 4–14 (2020).
  - [26] Sharon C. Glotzer, Dietrich Stauffer, and Naeem Jan, “Monte Carlo simulations of phase separation in chemically reactive binary mixtures,” *Physical Review Letters* **72**, 4109–4112 (1994).
  - [27] Sharon C. Glotzer, Edmund A. Di Marzio, and M. Muthukumar, “Reaction-Controlled Morphology of Phase-Separating Mixtures,” *Physical Review Letters* **74**, 2034–2037 (1995).
  - [28] Christoph A Weber, David Zwicker, Frank Jülicher, and Chiu Fan Lee, “Physics of active emulsions,” *Reports on Progress in Physics* **82**, 064601 (2019), 1806.09552.
  - [29] Yuting I Li and Michael E Cates, “Non-equilibrium phase separation with reactions: a canonical model and its behaviour,” *Journal of Statistical Mechanics: Theory and Experiment* **2020**, 053206 (2020), 2001.02563.
  - [30] Frank Jülicher and Christoph A. Weber, “Droplet Physics and Intracellular Phase Separation,” *Annual Review of Condensed Matter Physics* **15**, 237–261 (2023).
  - [31] Daniele Carati and René Lefever, “Chemical freezing of phase separation in immiscible binary mixtures,” *Physical Review E* **56**, 3127–3136 (1997).
  - [32] David Zwicker, Anthony A. Hyman, and Frank Jülicher, “Suppression of Ostwald ripening in active emulsions,” *Physical Review E* **92**, 012317 (2015).
  - [33] Jean David Wurtz and Chiu Fan Lee, “Chemical Reaction-Controlled Phase Separated Drops: Formation, Size Selection, and Coarsening,” *Physical Review Letters* **120**, 078102 (2018), 1707.08433.
  - [34] M. E. Cates, D. Marenduzzo, I. Pagonabarraga, and J. Tailleur, “Arrested phase separation in reproducing bacteria creates a generic route to pattern formation,” *Proceedings of the National Academy of Sciences* **107**, 11715–11720 (2010), 1001.0057.
  - [35] Dino Osmanović and Elisa Franco, “Chemical reaction motifs driving non-equilibrium behaviours in phase separating materials,” *Journal of the Royal Society Interface* **20**, 20230117 (2023), 2207.10135.
  - [36] Nirvana Caballero, Karsten Kruse, and Thierry Giamarchi, “Phase separation on surfaces in the presence of matter exchange,” *Physical Review E* **108**, L012801 (2023), 2205.03306.
  - [37] Jonathan Bauermann, Giacomo Bartolucci, Christoph A.

- Weber, and Frank Jülicher, “Theory of Reversed Ripening in Active Phase Separating Systems,” *Physical Review Letters* **135**, 148201 (2025).
- [38] Leonardo Demarchi, Andriy Goychuk, Ivan Maryshev, and Erwin Frey, “Enzyme-Enriched Condensates Show Self-Propulsion, Positioning, and Coexistence,” *Physical Review Letters* **130**, 128401 (2023), 2301.00392.
- [39] Gregor Häfner and Marcus Müller, “Reaction-Driven Diffusiophoresis of Liquid Condensates: Potential Mechanisms for Intracellular Organization,” *ACS Nano* **18**, 16530–16544 (2024).
- [40] Andriy Goychuk, Leonardo Demarchi, Ivan Maryshev, and Erwin Frey, “Self-consistent sharp interface theory of active condensate dynamics,” *Physical Review Research* **6**, 033082 (2024), 2401.17111.
- [41] Etienne Jambon-Puillet, Andrea Testa, Charlotta Lorenz, Robert W. Style, Aleksander A. Rebane, and Eric R. Dufresne, “Phase-separated droplets swim to their dissolution,” *Nature Communications* **15**, 3919 (2024).
- [42] David Zwicker, Rabea Seyboldt, Christoph A. Weber, Anthony A. Hyman, and Frank Jülicher, “Growth and division of active droplets provides a model for protocells,” *Nature Physics* **13**, 408–413 (2017), 1603.01571.
- [43] Florian Raßhofer, Simon Bauer, Alexander Ziepkke, Ivan Maryshev, and Erwin Frey, “Capillary wave formation in conserved active emulsions,” *Physical Review Research* **7**, 043240 (2025).
- [44] Arpan Kumar Rai, Jia-Xuan Chen, Matthias Selbach, and Lucas Pelkmans, “Kinase-controlled phase transition of membraneless organelles in mitosis,” *Nature* **559**, 211–216 (2018).
- [45] Mario Hofweber and Dorothee Dormann, “Friend or foe—Post-translational modifications as regulators of phase separation and RNP granule dynamics,” *Journal of Biological Chemistry* **294**, 7137–7150 (2019).
- [46] Izzy Owen and Frank Shewmaker, “The Role of Post-Translational Modifications in the Phase Transitions of Intrinsically Disordered Proteins,” *International Journal of Molecular Sciences* **20**, 5501 (2019).
- [47] Alan Mathison Turing, “The chemical basis of morphogenesis,” *Philosophical Transactions of the Royal Society of London. Series B, Biological Sciences* **237**, 37–72 (1952).
- [48] J. Halatek, F. Brauns, and E. Frey, “Self-organization principles of intracellular pattern formation,” *Philosophical Transactions of the Royal Society B: Biological Sciences* **373**, 20170107 (2018), 1802.07169.
- [49] Fridtjof Brauns, Jacob Halatek, and Erwin Frey, “Phase-Space Geometry of Mass-Conserving Reaction-Diffusion Dynamics,” *Physical Review X* **10**, 041036 (2020), 1812.08684.
- [50] Erwin Frey and Fridtjof Brauns, “Active Matter and Nonequilibrium Statistical Physics,” , 347–445 (2022).
- [51] Shiling Liang, Daniel Maria Busiello, and Paolo De Los Rios, “Emergent thermophoretic behavior in chemical reaction systems,” *New Journal of Physics* **24**, 123006 (2022), 2102.03197.
- [52] Timur Aslyamov, Francesco Avanzini, Étienne Fodor, and Massimiliano Esposito, “Nonideal Reaction-Diffusion Systems: Multiple Routes to Instability,” *Physical Review Letters* **131**, 138301 (2023), 2304.06394.
- [53] Lucas Menou, Chengjie Luo, and David Zwicker, “Physical interactions in non-ideal fluids promote Turing patterns,” *Journal of the Royal Society Interface* **20**, 20230244 (2023), 2302.12521.
- [54] Dino Osmanović and Elisa Franco, “Complex dynamics in reaction-phase separation systems,” *Physical Review E* **111**, 025404 (2025).
- [55] Florian Raßhofer and Erwin Frey, “Non-equilibrium phase coexistence in conserved chemically active mixtures,” (2026), (submitted).
- [56] Michael Rubinstein and Ralph H Colby, *Polymer Physics* (Oxford University Press, 2003).
- [57] Maurice L Huggins, “Solutions of Long Chain Compounds,” *The Journal of Chemical Physics* **9**, 440–440 (1941).
- [58] Paul J Flory, “Thermodynamics of High Polymer Solutions,” *The Journal of Chemical Physics* **10**, 51–61 (1942).
- [59] S.R. de Groot and P. Mazur, *Non-equilibrium Thermodynamics*, Dover Books on Physics (Dover Publications, 1984).
- [60] Lars Onsager, “Reciprocal Relations in Irreversible Processes. I,” *Physical Review* **37**, 405–426 (1930); “Reciprocal Relations in Irreversible Processes. II.” *Physical Review* **38**, 2265–2279 (1931).
- [61] Hao Dong, Sanbo Qin, and Huan-Xiang Zhou, “Effects of Macromolecular Crowding on Protein Conformational Changes,” *PLoS Computational Biology* **6**, e1000833 (2010).
- [62] Jitao Wen, Liu Hong, Georg Krainer, Qiong-Qiong Yao, Tuomas P. J. Knowles, Si Wu, and Sarah Perrett, “Conformational Expansion of Tau in Condensates Promotes Irreversible Aggregation,” *Journal of the American Chemical Society* **143**, 13056–13064 (2021).
- [63] Rif Harris, Nofar Berman, and Ayala Lampel, “Coacervates as enzymatic microreactors,” *Chemical Society Reviews* **54**, 4183–4199 (2025).
- [64] Brian G. O’Flynn and Tanja Mittag, “The role of liquid–liquid phase separation in regulating enzyme activity,” *Current Opinion in Cell Biology* **69**, 70–79 (2021).
- [65] Quan-Xing Liu, Arjen Doelman, Vivi Rottschäfer, Monique de Jager, Peter M. J. Herman, Max Rietkerk, and Johan van de Koppel, “Phase separation explains a new class of self-organized spatial patterns in ecological systems,” *Proceedings of the National Academy of Sciences* **110**, 11905–11910 (2013).
- [66] Xiongfei Fu, Lei-Han Tang, Chenli Liu, Jian-Dong Huang, Terence Hwa, and Peter Lenz, “Stripe Formation in Bacterial Systems with Density-Suppressed Motility,” *Physical Review Letters* **108**, 198102 (2012), 1204.0615.
- [67] M. C. Cross and P. C. Hohenberg, “Pattern formation outside of equilibrium,” *Reviews of Modern Physics* **65**, 851–1112 (1993).
- [68] A. J. Bray, “Theory of phase-ordering kinetics,” *Advances in Physics* **51**, 481–587 (2002).
- [69] See Supplemental Material at URL-to-be-inserted-by-the-publisher for details of the numerical methods and for a discussion of an alternative reaction scheme; including Refs. [49, 50, 55, 71, 72, 87–89].
- [70] Michael Cross and Henry Greenside, *Pattern Formation and Dynamics in Nonequilibrium Systems* (Cambridge University Press, 2009).
- [71] Fridtjof Brauns, Henrik Weyer, Jacob Halatek, Junghoon Yoon, and Erwin Frey, “Wavelength Selection by Interrupted Coarsening in Reaction-Diffusion Systems,” *Phys-*

- ical Review Letters **126**, 104101 (2021), 2005.01495.
- [72] Henrik Weyer, Fridtjof Brauns, and Erwin Frey, “Coarsening and wavelength selection far from equilibrium: A unifying framework based on singular perturbation theory,” *Physical Review E* **108**, 064202 (2023), 2203.03892.
- [73] Carsten Donau and Job Boekhoven, “The chemistry of chemically fueled droplets,” *Trends in Chemistry* **5**, 45–60 (2023).
- [74] Xiaolei Su, Jonathon A. Ditlev, Enfu Hui, Wenmin Xing, Sudeep Banjade, Julia Okrut, David S. King, Jack Taunton, Michael K. Rosen, and Ronald D. Vale, “Phase separation of signaling molecules promotes T cell receptor signal transduction,” *Science* **352**, 595–599 (2016).
- [75] Sudeep Banjade and Michael K. Rosen, “Phase transitions of multivalent proteins can promote clustering of membrane receptors,” *eLife* **3**, e04123 (2014).
- [76] Alena Khmelinskaia, Henri G. Franquelim, Eugene P. Petrov, and Petra Schwille, “Effect of anchor positioning on binding and diffusion of elongated 3D DNA nanostructures on lipid membranes,” *Journal of Physics D: Applied Physics* **49**, 194001 (2016).
- [77] Alena Khmelinskaia, Jonas Mücksch, Eugene P. Petrov, Henri G. Franquelim, and Petra Schwille, “Control of Membrane Binding and Diffusion of Cholesteryl-Modified DNA Origami Nanostructures by DNA Spacers,” *Langmuir* **34**, 14921–14931 (2018).
- [78] Jefferson D. Knight, Michael G. Lerner, Joan G. Marcano-Velázquez, Richard W. Pastor, and Joseph J. Falke, “Single Molecule Diffusion of Membrane-Bound Proteins: Window into Lipid Contacts and Bilayer Dynamics,” *Biophysical Journal* **99**, 2879–2887 (2010).
- [79] Brian P. Ziemba and Joseph J. Falke, “Lateral diffusion of peripheral membrane proteins on supported lipid bilayers is controlled by the additive frictional drags of (1) bound lipids and (2) protein domains penetrating into the bilayer hydrocarbon core,” *Chemistry and Physics of Lipids* **172**, 67–77 (2013).
- [80] P. G. Saffman and M. Delbrück, “Brownian motion in biological membranes.” *Proceedings of the National Academy of Sciences* **72**, 3111–3113 (1975).
- [81] Matti Javanainen, Hector Martinez-Seara, Ralf Metzler, and Ilpo Vattulainen, “Diffusion of Integral Membrane Proteins in Protein-Rich Membranes,” *The Journal of Physical Chemistry Letters* **8**, 4308–4313 (2017).
- [82] Hong Jiang, Xiaoyu Zhang, Xiao Chen, Pornpun Aramsangtienchai, Zhen Tong, and Hening Lin, “Protein Lipidation: Occurrence, Mechanisms, Biological Functions, and Enabling Technologies,” *Chemical Reviews* **118**, 919–988 (2018).
- [83] Erik E. Griffin, David J. Odde, and Geraldine Seydoux, “Regulation of the MEX-5 Gradient by a Spatially Segregated Kinase/Phosphatase Cycle,” *Cell* **146**, 955–968 (2011).
- [84] Johan van de Koppel, Joanna C. Gascoigne, Guy Theraulaz, Max Rietkerk, Wolf M. Mooij, and Peter M. J. Herman, “Experimental Evidence for Spatial Self-Organization and Its Emergent Effects in Mussel Bed Ecosystems,” *Science* **322**, 739–742 (2008).
- [85] A. Y. Grosberg and J.-F. Joanny, “Nonequilibrium statistical mechanics of mixtures of particles in contact with different thermostats,” *Physical Review E* **92**, 032118 (2015).
- [86] Simon N. Weber, Christoph A. Weber, and Erwin Frey, “Binary Mixtures of Particles with Different Diffusivities Demix,” *Physical Review Letters* **116**, 058301 (2016), 1505.00525.
- [87] Wolfram Research Inc., “Mathematica,” *Champaign, Illinois* (2024).
- [88] COMSOL AB, “COMSOL Multiphysics® v. 6.1,” *Stockholm* (2023).
- [89] Florian Raßhofer and Erwin Frey, “Local composition controls pattern formation in conserved active emulsions – Additional material,” *Zenodo* (2025), 10.5281/zenodo.17790391, digital repository containing Comsol simulation files and Mathematica notebooks used for linear stability analysis and the sharp-interface theory.